

# Quasiliving Cationic Polymerization of Styrene and Isobutylene: Run Number and Apparent Rate Constant of Ionization by $\text{TiCl}_4$ and Energies of Activation of Elementary Reactions

Quinn A. Smith and Robson F. Storey\*

The University of Southern Mississippi, School of Polymers and High Performance Materials, Box 10076, Hattiesburg, Mississippi 39406

Received March 6, 2005; Revised Manuscript Received April 8, 2005

**ABSTRACT:** The quantity  $k_p/k_{-i}$  was measured from first-order kinetic data for cationic quasiliving polymerization of styrene and isobutylene initiated with 5-*tert*-butyl-1,3-bis(2-chloro-2-propyl)benzene (bDCC)/ $\text{TiCl}_4$  in 60/40 MCHex/MeCl, via analysis of an initiation event termed rapid monomer consumption (RMC). RMC is characterized by an initial period of high polymerization rate followed by slower first-order decay in monomer concentration and is due to a larger ionization rate for the initiator compared to the polymer chain end. The value of  $k_p/k_{-i}$  was used in conjunction with the apparent rate constant for propagation,  $k_{\text{app}}$ , to calculate apparent rate constants of chain-end ionization,  $k_i$ , for both monomers at  $-60$ ,  $-70$ ,  $-80$ , and  $-90$  °C, independently of  $k_p$ . Rate constants of ion-pair collapse and ionization equilibrium were calculated assuming published values of  $k_p$ . Apparent energies of activation for  $k_p/k_{-i}$  of  $-2.4$  and  $-4.6$  kcal/mol were determined for styrene and IB, respectively. Apparent energies of activation for ionization, propagation, and ionization equilibrium were calculated for both monomers. Rates of chain-end ionization and ion-pair collapse were both higher and more sensitive to temperature for polyisobutylene than polystyrene.

## Introduction

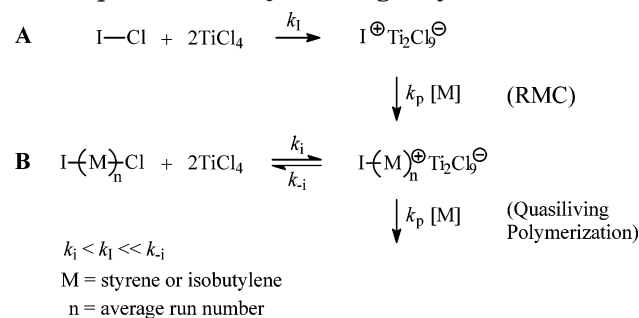
Real-time ATR–FTIR reaction monitoring has afforded a more in-depth mechanistic view of initiation and propagation processes for styrene and isobutylene (IB) quasiliving carbocationic polymerizations.<sup>1–4</sup> These polymerizations proceed through an ionization equilibrium between reversibly terminated (dormant) chain ends and actively propagating carbocations, as illustrated at **B** in Scheme 1, for ionization by  $\text{TiCl}_4$ .<sup>5,6</sup> Run number (RN) is defined as the average number of monomer units added during one ionization–termination cycle,<sup>7</sup> at a given monomer concentration,  $[\text{M}]$ . In the absence of transfer reactions RN is determined by the ratio of the rate of propagation to the rate of reversible termination, as shown in eq 1

$$\text{RN} = \frac{k_p[\text{M}]}{k_{-i}} \quad (1)$$

where  $k_p$  is the absolute rate constant for propagation of paired ions and  $k_{-i}$  is the rate constant of ion-pair collapse. Referring to Scheme 1 at **A**, the first run of monomer originates from the initiating cation. If the rate constant for ionization of the initiator,  $k_i$ , is larger than that of the chain end,  $k_{-i}$ , a phenomenon termed rapid monomer consumption (RMC) is observed. We have shown<sup>8,9</sup> that RMC provides a way to measure the number of monomer units consumed in this first run, which, when combined with the known concentration of growing chains, provides a measure of the quantity  $k_p/k_{-i}$ .

RMC is characterized by a transient period of high polymerization rate observed immediately upon initiation, followed by slower first-order polymerization. RMC is observed for styrene<sup>8,9</sup> and isobutylene<sup>8,10</sup> (IB) polymerizations initiated with 5-*tert*-butyl-1,3-bis(2-chloro-2-propyl)benzene (bDCC)/ $\text{TiCl}_4$  in 60/40 methylecyclo-

## Scheme 1. Mechanism of Quasiliving Carbocationic Polymerization: (A) Ionization of Initiator and Rapid Monomer Consumption (RMC); (B) Ionization Equilibrium of Quasiliving Polymerization



hexane/methyl chloride (MCHex/MeCl), as represented in Figure 1 for both monomers. These plots show a well-defined point, associated with a sharp decrease in slope, at which the initiating cations are exhausted and the equilibrium concentration of chain ends becomes established. Because of the relative infrequency of polymer chain-end ionization under these conditions,<sup>8,11</sup> it can be assumed that all initiating sites undergo one ionization–propagation–termination cycle before any significant number of second ionizations occurs. Thus, the monomer concentration consumed during RMC,  $[\text{M}]_{\text{RMC}}$ , divided by the concentration of initiating sites,  $[\text{I}]_0$ , yields the average run number,  $\overline{\text{RN}}$ , for the initiating cations, which is proportional to the average monomer concentration during RMC, according to eq 1. As long as the monomer concentration remains relatively constant and approximately equal to  $[\text{M}]_0$ , i.e.,  $[\text{M}]_{\text{RMC}}/[\text{M}]_0 \leq 0.10$ , this approach can be used to measure  $k_p/k_{-i}$ .

To obtain the quantity  $k_p/k_{-i}$  under conditions of moderate to high monomer conversion, we recently derived<sup>9</sup> an integrated form of eq 1 for the RMC period. Insertion of boundary conditions at the end of the RMC

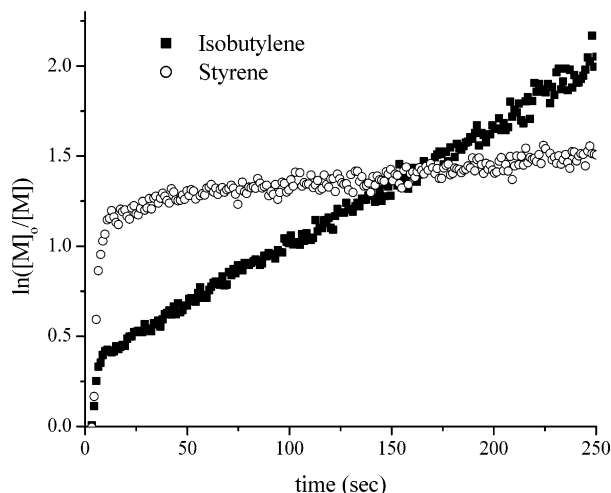


**Figure 1.** First-order plots for styrene and isobutylene polymerization initiated by bDCC.  $[\text{TiCl}_4] = 2.78 \times 10^{-2} \text{ M}$ ;  $[\text{styrene}]_0 = [\text{IB}]_0 = 0.5 \text{ M}$ ;  $[\text{bDCC}]_0 = 8.0 \times 10^{-3} \text{ M}$ ;  $[\text{DtBP}] = 4.0 \times 10^{-3} \text{ M}$ ;  $[\text{n-Bu}_4\text{NCl}] = 5.0 \times 10^{-4} \text{ M}$ ; 60/40 MCHex/MeCl cosolvents (v/v),  $-90^\circ \text{C}$ .

period yielded eq 2, where the monomer concentration remaining,  $[\text{M}]_r$ , is equal to  $([\text{M}]_0 - [\text{M}]_{\text{RMC}})$ , and the number of polymer chains created,  $[\text{P}]$ , equals  $[\text{I}]_0$ . Equation 2 allows calculation of the quantity  $k_p/k_{-i}$  from  $[\text{M}]_{\text{RMC}}$  data when  $[\text{M}]_{\text{RMC}}/[\text{M}]_0 > 0.10$ , i.e., when a significant fraction of the monomer is consumed during RMC.

$$\frac{k_p}{k_{-i}} = \frac{1}{[\text{I}]_0} \ln \frac{[\text{M}]_0}{[\text{M}]_0 - [\text{M}]_{\text{RMC}}} = \frac{1}{[\text{I}]_0} \ln \frac{[\text{M}]_0}{[\text{M}]_r} \quad (2)$$

We originally calculated<sup>8</sup>  $k_p/k_{-i}$  at  $[\text{M}]_0 = 0.5 \text{ M}$  for styrene at  $-70^\circ \text{C}$  by extrapolating RN, obtained from  $[\text{M}]_{\text{RMC}}/[\text{I}]_0$ , to infinite initiator dilution, as we suspected that chain transfer to initiator, "inifering", was in play. This yielded  $k_p/k_{-i}$  at  $-70^\circ \text{C}$  of 78 and  $9.4 \text{ M}^{-1}$  for styrene and IB, respectively. Further analysis of this process resulted in direct calculation of apparent rate constants of chain-end ionization ( $k_i$ , Scheme 1 at B) of 1.3 and  $15 \text{ M}^{-2} \text{ s}^{-1}$ . The  $k_i$  values agreed remarkably well with recent results reported by Faust et al. of 4.2 and  $16.4 \text{ M}^{-2} \text{ s}^{-1}$  for styrene<sup>12</sup> and isobutylene,<sup>11</sup> respectively. A later, more rigorous determination of  $k_p/k_{-i}$  using eq 2 led to values of  $k_p/k_{-i} = 63 \text{ M}^{-1}$  and  $k_i = 1.2 \text{ M}^{-2} \text{ s}^{-1}$  for styrene at  $-70^\circ \text{C}$ .<sup>9</sup>

After reporting calculation of the apparent rate constant of ionization for styrene and isobutylene at  $-70^\circ \text{C}$ , we sought to determine  $k_i$  for both monomers over a range of temperatures and thereby calculate the apparent energy of activation for ionization.  $k_i$  is an apparent rate constant in  $\text{TiCl}_4$ -co-initiated quasiling polymerizations due to the ionization of chain ends by  $\text{Ti}_2\text{Cl}_6$ .<sup>11</sup> Therefore, the apparent rate constant of ionization is defined as  $k_{\text{iabs}}K_{\text{D0}}$ , where  $k_{\text{iabs}}$  is the absolute rate constant of ionization and  $K_{\text{D0}}$  is the equilibrium dimerization constant for  $\text{TiCl}_4$ . Because dimerization of  $\text{TiCl}_4$  is an exothermic process,<sup>13</sup> as temperature decreases  $K_{\text{D0}}$  increases while  $k_{\text{iabs}}$  decreases. Therefore, a larger energy of activation for  $\text{TiCl}_4$  dimerization relative to that of ionization could result in a negative apparent activation energy for ionization.

The apparent activation energy for propagation for quasiling cationic polymerizations,  $E_{\text{app}}$ , has been consistently found to be negative for styrene and IB

polymerizations using  $\text{TiCl}_4$  co-initiator.<sup>4,14–17</sup> Recent studies found the rate of propagation of IB and styrene monomers to be diffusion-controlled at low temperature,<sup>11,12,18,19</sup> i.e., the energy of activation for propagation,  $E_p$ , is negligible. In light of this and the absence of chain transfer reactions in quasiling polymerization systems, the apparent activation energy for the polymerization process may be defined as  $E_{\text{app}} \cong E_i - E_{-i}$ , where  $E_{-i}$  is the activation energy for ion-pair collapse and  $E_i$  is the apparent activation energy of chain-end ionization. If  $E_{\text{app}} < 0$ , assuming both  $E_i$  and  $E_{-i}$  are positive, it would appear that ion-pair collapse must be more sensitive to changes in temperature than chain-end ionization. However,  $E_{\text{app}} < 0$  would also result if  $E_i$  is negative, the possibility of which was described above.

The focus of this work is determination of the apparent activation energy for RN ( $k_p/k_{-i}$ ) and ionization by  $\text{TiCl}_4$  ( $k_i$ ) for styrene and IB from  $-60$  to  $-90^\circ \text{C}$  independently of assumed values of  $k_p$ . Also important is calculation of apparent activation energy for rate constants of ion-pair collapse and ionization equilibrium constants for both monomers.

## Experimental Section

**Materials.** Isobutylene and methyl chloride (Matheson Gases) were dried by passing the gas through a column packed with  $\text{CaSO}_4$  or  $\text{CaSO}_4/4 \text{ \AA}$  molecular sieves, respectively. Styrene (99%, Aldrich) and 2,6-di-*tert*-butylpyridine (97%, Aldrich) were freshly distilled over  $\text{CaH}_2$ . Titanium tetrachloride (99%, Aldrich) was freshly distilled. Synthesis of bDCC has been previously reported.<sup>14</sup> Anhydrous methylcyclohexane (99+%, Aldrich) and tetra-*n*-butylammonium chloride (99+%, Fluka) were used as received.

**Instrumentation.** A ReactIR 4000 reaction analysis system (light conduit type) (ASI Applied Systems, Millersville, MD) equipped with a DiComp (diamond composite) insertion probe, a general purpose type PR-11 platinum resistance thermometer (RTD), and a CN76000 series temperature controller (Omega Engineering, Stamford, CT) was used to collect infrared spectra of the polymerization components in real time. Number- ( $M_n$ ) and weight-average ( $M_w$ ) molecular weights and polydispersity index (PDI,  $M_w/M_n$ ) were determined using a gel permeation chromatography (GPC) system equipped with a Wyatt Technology mini-DAWN on-line MALLS detector, as previously described.<sup>20</sup>

**Procedures.** Polymerizations were carried out within a glovebox, equipped with an integral, cryostated heptane bath. Initial concentrations of monomer (0.5 M), Lewis base ( $[\text{DtBP}] = 4.0 \times 10^{-3} \text{ M}$ ), co-initiator ( $[\text{TiCl}_4] = 2.78 \times 10^{-2} \text{ M}$ ), and common ion salt precursor ( $[\text{n-Bu}_4\text{NCl}] = 5.0 \times 10^{-4} \text{ M}$ ), cosolvent composition (MCHex/MeCl 60/40, v/v), and reaction volume (200 mL) were held constant in all cases, and  $\text{TiCl}_4$  was the final component added. The following was a typical polymerization procedure. The DiComp probe was fitted into a dry 250 mL four-necked round-bottomed flask equipped with a mechanical stirrer and RTD and immersed into the cold heptane bath ( $-70^\circ \text{C}$ ) where it was allowed to thermally equilibrate prior to acquisition of a background spectrum (128 scans,  $8 \text{ cm}^{-1}$  resolution). To the chilled flask were added sequentially  $1.64 \times 10^{-3} \text{ mol}$  (0.471 g) bDCC and 188 mL of a stock solution prepared from  $4.8 \times 10^{-3} \text{ mol}$  (1.08 mL) of DtBP,  $6 \times 10^{-4} \text{ mol}$  (0.167 g) of *n*- $\text{Bu}_4\text{NCl}$ , 676 mL of MCHex, and 450 mL of MeCl. The solvents were equilibrated at the reaction temperature prior to formulating the stock solution. The reaction mixture was stirred until it reached thermal equilibrium as indicated by the RTD. Subsequently, 0.10 mol (11.5 mL) of styrene (room temperature) was added, and the mixture was again allowed to reach thermal equilibrium. After stirring for an additional 5 min,  $5.6 \times 10^{-3} \text{ mol}$  (0.61 mL) of  $\text{TiCl}_4$ , neat and at room temperature, was rapidly injected into the

Table 1. bDCC-Initiated Styrene and IB Run Number and Rate Constant Data,  $-60\text{ }^{\circ}\text{C}^a$ 

$[\text{bDCC}] \times 10^3, \text{M}$	$[\text{M}]_{\text{RMC}}$	$k_p/k_{-i}, \text{M}^{-1}$	$\overline{\text{RN}}$	corr $k_{\text{app}} \times 10^4, \text{s}^{-1}$	$k_p k_i/k_{-i}, \text{M}^{-2} \text{s}^{-1}$	$k_i, \text{M}^{-2} \text{s}^{-1}$	$\Delta T_{\text{max}}, ^{\circ}\text{C}$
Styrene, $-60\text{ }^{\circ}\text{C}$							
8.0	0.21	34.4	26.4	8.7	71	2.1	7.2
7.3	0.20	35.6	27.8	6.8	60	1.7	6.7
6.0	0.18	37.5	30.2	4.9	53	1.4	5.2
5.0	0.16	39.0	32.3	4.1	54	1.4	5.1
4.1	0.14	41.5	35.2	4.5	71	1.7	4.8
3.6	0.13	42.3	36.5	3.6	65	1.5	4.6
3.1	0.11	41.8	36.8	3.2	66	1.6	3.8
2.6	0.10	42.3	38.0	2.8	70	1.6	3.6
Isobutylene, $-60\text{ }^{\circ}\text{C}$							
14.0	0.057	4.3	4.0	6.9	32	7.5	1.8
12.0	0.050	4.4	4.2	6.5	35	8.0	1.7
10.0	0.043	4.5	4.3	5.5	35	7.9	1.4
8.0	0.033	4.3	4.2	4.9	40	9.3	1.3
6.0	0.025	4.3	4.2	3.7	40	9.3	1.0
4.0	0.017	4.4	4.3	2.5	40	9.2	1.1
2.0	0.008	4.3	4.2	1.4	46	10.9	0.8
1.0	0.004	4.2	4.2	0.6	38	9.1	0.6

<sup>a</sup>  $[\text{Styrene}]_0$  (or  $[\text{IB}]_0$ ) = 0.5 M,  $[\text{DtBP}] = 4.0 \times 10^{-3}$  M,  $[\text{n-Bu}_4\text{NCl}] = 5.0 \times 10^{-4}$  M, and  $[\text{TiCl}_4] = 2.78 \times 10^{-2}$  M; 60/40 MCHex/MeCl cosolvents (v/v).

reactor. The polymerizations were terminated at about 380 s by addition of 5 mL of methanol to the reaction flask.

Reaction conversion was determined by monitoring the intensity of the absorbance (integrated peak area) centered around 907 and 887  $\text{cm}^{-1}$  associated with the  $=\text{CH}_2$  wag of styrene and IB, respectively. The rapid acquisition mode of the ReactIR 4000 was used to collect IR spectra of the reaction medium for 200 s (1.4 spectra/s, 2 scans/spectrum, 4  $\text{cm}^{-1}$  resolution) prior to and after monomer addition to obtain solvent reference,  $A_r$ , and initial monomer concentration,  $A_0$ , absorbance values. The value obtained for  $A_r$  was then reduced by 6 or 8% for IB and styrene, respectively, which accounts for the volume dilution, and thus the solvent absorbance reduction, caused by subsequent addition of monomer and  $\text{TiCl}_4$ . A third set of spectra was acquired of the polymerization medium for 428 s, 0.93 spectra/s (2 scans/spectrum, 4  $\text{cm}^{-1}$  resolution);  $\text{TiCl}_4$  was introduced at 50 s, and finally methanol was added immediately after collection of the last spectrum. Each spectrum was collected over the spectral ranges 4000–2200 and 1900–650  $\text{cm}^{-1}$ . The absorbance of the peaks associated with the  $=\text{CH}_2$  wag of IB and styrene monomer is known to decrease with increasing temperature by a factor of  $\sim 0.42\%/^{\circ}\text{C}$ .<sup>10</sup> To account for reaction exotherm during the polymerization, a spectroscopic correction for temperature was made. Thus, absorbance data were converted to relative monomer concentrations using the following relationship

$$\frac{[\text{M}]_0}{[\text{M}]_t} = \frac{A_0 - A_r}{(A_t - A_r)(1 + 0.0042\Delta T)} \quad (3)$$

where  $[\text{M}]_t$  and  $A_t$  are the monomer concentration and absorbance, respectively, at time  $t$ , and  $\Delta T$  is the difference between the actual temperature of the reactor contents and the nominal temperature of the experiment. Temperature data were taken manually.

The concentration of monomer consumed during the RMC,  $[\text{M}]_{\text{RMC}}$ , was measured by calculating  $[\text{M}]$  at the point of intersection of the two linear regions observed in first-order kinetic plots, one of which occurs during RMC and one immediately thereafter, as shown in Figure 1.

## Results and Discussion

**Determination of  $k_p/k_{-i}$ .** RMC was observed in both styrene and IB quasiling polymerizations using the 5-*tert*-butyl-1,3-bis(2-chloro-2-propyl)benzene (bDCC)/ $\text{TiCl}_4$  initiating system in MCHex/MeCl 60/40 (v/v). The values of  $k_p/k_{-i}$  for styrene and IB polymerizations run at  $-60$ ,  $-70$ ,  $-80$ , and  $-90\text{ }^{\circ}\text{C}$  were measured according

to eq 2 using  $[\text{M}]_{\text{RMC}}$  values obtained from first-order plots. A series of  $[\text{bDCC}]_0$  was employed for each temperature for both monomers, and the following conditions remained constant:  $[\text{styrene}]_0$  (or  $[\text{IB}]_0$ ) = 0.5 M;  $[\text{DtBP}] = 4.0 \times 10^{-3}$  M;  $[\text{n-Bu}_4\text{NCl}] = 5.0 \times 10^{-4}$  M, and  $[\text{TiCl}_4] = 2.78 \times 10^{-2}$  M.

Tables 1–4 list initial concentrations of  $[\text{bDCC}]$ ,  $[\text{M}]_{\text{RMC}}$ ,  $\overline{\text{RN}}$ ,  $k_p/k_{-i}$ , and reaction exotherms, for both monomers for  $-60$ ,  $-70$ ,  $-80$ , and  $-90\text{ }^{\circ}\text{C}$ , respectively. Values of  $k_p/k_{-i}$  for styrene are significantly larger than those for IB: 3 times larger at  $-90\text{ }^{\circ}\text{C}$  and 10 times larger at  $-60\text{ }^{\circ}\text{C}$  for  $[\text{bDCC}]_0 = 8 \times 10^{-3}$  M. Because  $k_p$  has been found to be near the diffusion limit for both monomers,<sup>11,12</sup>  $k_{-i}(\text{IB})$  appears to be larger than  $k_{-i}(\text{S})$ ; i.e., ion-pair collapse is faster in the IB polymerization. Thus, monomer conversion during RMC is higher for styrene than for isobutylene, given the same concentration of initiating cations for both monomers. Specifically, at  $-60\text{ }^{\circ}\text{C}$  for  $[\text{bDCC}]_0 = 8 \times 10^{-3}$  M,  $[\text{M}]_{\text{RMC}}(\text{S})$  is 6 times greater than  $[\text{M}]_{\text{RMC}}(\text{IB})$ . As expected with high monomer conversion during RMC for styrene polymerizations, significant reaction exotherms accompanied initiation. For example, at  $-90\text{ }^{\circ}\text{C}$ , where  $[\text{bDCC}]_0 = 8.0 \times 10^{-3}$  M, the temperature rose 11.3  $^{\circ}\text{C}$  during the first 30 s of the polymerization. Under identical conditions for IB the temperature rose 5.8  $^{\circ}\text{C}$  and did not maximize until 2 min into the polymerization. Rises in temperature during these polymerizations change the kinetics of both ionization and ion-pair collapse. For our purposes, it was important to calculate  $k_p/k_{-i}$  for constant reaction temperatures of  $-60$ ,  $-70$ ,  $-80$ , and  $-90\text{ }^{\circ}\text{C}$ . We chose to accept values of  $k_p/k_{-i}$  for further kinetic analysis only from polymerizations where the reaction exotherm,  $\Delta T$ , was  $<5\text{ }^{\circ}\text{C}$ . The sole exception was  $[\text{bDCC}] = 2 \times 10^{-3}$  M for styrene at  $-90\text{ }^{\circ}\text{C}$ , for which  $\Delta T$  was 6.1  $^{\circ}\text{C}$ . The average temperature rise during RMC can be no higher than  $1/2(\Delta T)$ , and in most cases it was considerably less than this; therefore, we are confident that this criterion is appropriate.

Molecular weight data for all reactions are summarized in the Supporting Information. Most notable in these data were the consistently higher PDIs for styrene polymerizations relative to IB polymerizations. The higher PDIs for styrene polymerizations were attributed to higher RNs observed for styrene polymerizations relative to IB polymerizations.



Table 2. bDCC-Initiated Styrene and IB Run Number and Rate Constant Data,  $-70\text{ }^{\circ}\text{C}^a$ 

$[\text{bDCC}] \times 10^3, \text{M}$	$[\text{M}]_{\text{RMC}}$	$k_p/k_{-i}, \text{M}^{-1}$	$\overline{\text{RN}}$	$\text{corr } k_{\text{app}} \times 10^4, \text{s}^{-1}$	$k_p k_i/k_{-i}, \text{M}^{-3} \text{s}^{-1}$	$k_i, \text{M}^{-2} \text{s}^{-1}$	$\Delta T_{\text{max}}, ^{\circ}\text{C}$
Styrene, $-70\text{ }^{\circ}\text{C}$							
8.2	0.27	46.1	32.3	11.5	91	2.0	10.7
6.6	0.24	50.0	36.6	11.3	111	2.2	9.9
5.0	0.21	54.5	42.0	8.3	108	2.0	7.8
5.0	0.20	51.0	40.0	6.7	86	1.7	7.9
3.4	0.17	60.3	49.5	5.5	105	1.7	6.7
3.0	0.15	57.3	48.5	4.9	105	1.8	6.0
1.8	0.11	67.5	59.9	3.9	140	2.1	4.4
1.5	0.10	71.6	64.4	2.6	111	1.6	3.9
Isobutylene, $-70\text{ }^{\circ}\text{C}$							
14.6	0.11	8.6	7.6	36.8	163	19.1	3.7
13.0	0.11	9.1	8.1	36.4	181	19.9	3.8
12.0	0.12	11.3	9.9	18.6	100	8.9	2.3
11.4	0.10	9.5	8.5	30.0	170	18.0	3.1
9.8	0.09	10.0	9.1	26.2	173	17.3	2.5
9.0	0.07	8.3	7.7	14.4	104	12.4	2.0
8.2	0.08	10.1	9.3	22.5	177	17.6	2.3
6.6	0.06	9.8	9.2	16.9	165	16.8	2.1
5.0	0.04	8.5	8.1	8.2	106	12.5	1.3
3.5	0.03	9.7	9.4	5.5	101	10.4	1.2
2.0	0.02	10.0	9.8	3.5	113	11.3	0.9
0.9	0.01	8.9	8.8	1.5	108	12.1	0.4

<sup>a</sup>  $[\text{Styrene}]_0$  (or  $[\text{IB}]_0$ ) = 0.5 M,  $[\text{DtBP}] = 4.0 \times 10^{-3} \text{ M}$ ,  $[\text{n-Bu}_4\text{NCl}] = 5.0 \times 10^{-4} \text{ M}$ , and  $[\text{TiCl}_4] = 2.78 \times 10^{-2} \text{ M}$ ; 60/40 MCHex/MeCl cosolvents (v/v).

Table 3. bDCC-Initiated Styrene and IB Run Number and Rate Constant Data,  $-80\text{ }^{\circ}\text{C}^a$ 

$[\text{bDCC}] \times 10^3, \text{M}$	$[\text{M}]_{\text{RMC}}$	$k_p/k_{-i}, \text{M}^{-1}$	$\overline{\text{RN}}$	$\text{corr } k_{\text{app}} \times 10^4, \text{s}^{-1}$	$k_p k_i/k_{-i}, \text{M}^{-3} \text{s}^{-1}$	$k_i, \text{M}^{-2} \text{s}^{-1}$	$\Delta T_{\text{max}}, ^{\circ}\text{C}$
Styrene, $-80\text{ }^{\circ}\text{C}$							
9.0	0.31	53.2	34.2	12.4	89	1.7	11.1
8.0	0.29	53.2	35.8	12.9	104	2.0	11.2
7.0	0.28	57.4	39.5	12.7	117	2.0	9.5
6.0	0.25	58.6	42.1	9.4	102	1.7	8.0
5.0	0.23	61.6	46.0	10.5	136	2.2	8.7
4.0	0.21	69.5	53.3	8.3	135	1.9	6.2
3.0	0.18	76.8	61.5	7.4	161	2.1	6.5
2.0	0.14	80.3	68.6	4.7	152	1.9	5.4
1.0	0.08	93.0	84.9	3.7	241	2.6	3.5
0.7	0.06	89.3	84.0	2.0	187	2.1	2.6
Isobutylene, $-80\text{ }^{\circ}\text{C}$							
14.0	0.15	12.3	10.4	60.6	280	22.7	4.1
12.0	0.12	11.2	9.8	48.6	262	23.5	4.0
10.0	0.11	12.1	10.8	39.6	256	21.1	3.4
8.0	0.084	11.6	10.6	32.0	259	22.3	3.1
6.0	0.07	13.5	12.5	23.3	251	18.6	2.7
4.0	0.05	14.1	13.4	14.9	241	17.0	2.1
2.0	0.03	13.0	12.7	7.2	233	17.9	1.4

<sup>a</sup>  $[\text{Styrene}]_0$  (or  $[\text{IB}]_0$ ) = 0.5 M,  $[\text{DtBP}] = 4.0 \times 10^{-3} \text{ M}$ ,  $[\text{n-Bu}_4\text{NCl}] = 5.0 \times 10^{-4} \text{ M}$ , and  $[\text{TiCl}_4] = 2.78 \times 10^{-2} \text{ M}$ ; 60/40 MCHex/MeCl cosolvents (v/v).

**Rate Constant Determination.** In Tables 1-4, the values of  $k_p/k_{-i}$  for which  $\Delta T < 5\text{ }^{\circ}\text{C}$  were averaged for each temperature, and the average values are reported in Table 5. Using reported values of  $k_p$  for IB<sup>11</sup> and styrene<sup>12</sup> of  $7 \times 10^8$  and  $1.5 \times 10^9 \text{ M}^{-1} \text{s}^{-1}$ , respectively, values of  $k_{-i}$  were calculated and are also reported in Table 5. Values of  $k_{-i}$  decrease with decreasing temperature for both monomers, as expected. Also, as mentioned above, values of  $k_{-i}$  are larger for IB than styrene at each temperature, e.g., by a factor of 6 at  $-60\text{ }^{\circ}\text{C}$  and of 3 at  $-90\text{ }^{\circ}\text{C}$ , indicating that the lifetime of ionization for the active PS chain end is larger than for the active PIB chain end, experimentally observed by the higher  $[\text{M}]_{\text{RMC}}$  for styrene. Because the ratio  $k_{-i}^{\text{IB}}/k_{-i}^{\text{S}}$  decreases with decreasing temperature, it appears as though  $k_{-i}^{\text{IB}}$  is more sensitive to temperature than  $k_{-i}^{\text{S}}$  and must have a larger positive energy of activation.

As Figure 1 illustrates, under identical conditions, the post-RMC slope of the first-order plot,  $k_{\text{app}}$ , is higher for IB than for styrene, and we can conclude that  $k_p k_i/k_{-i}$

for the PIB chain end is greater than that for the PS chain end under these conditions, according to eq 4, where  $k_i/k_{-i}$  is the ionization equilibrium constant of the chain ends (Scheme 1 at **B**). Interestingly, even though the slope of the first-order plot is higher for IB than for styrene, i.e., the propagation rate of IB is higher, the monomer conversion before the reaction time of 175 s is higher for styrene due to its larger RN and larger degree of RMC. Therefore, without real-time FTIR to see the details of initiation it would appear as though IB were propagating more slowly than styrene during this period, which would be inaccurate.

$$k_{\text{app}} = k_p[\text{R}^+\text{Ti}_2\text{Cl}_9^-] \cong \frac{k_p}{k_{-i}} k_i[\text{I}]_0[\text{TiCl}_4]^2 \quad (4)$$

According to eq 4, the apparent rate constant of propagation for quasiliving polymerizations is directly proportional to  $k_p k_i/k_{-i}$ , where  $k_i$  is the apparent rate constant of ionization. A larger slope in first-order plots

Table 4. bDCC-Initiated Styrene and IB Run Number and Rate Constant Data,  $-90\text{ }^{\circ}\text{C}^a$ 

$[\text{bDCC}] \times 10^3, \text{M}$	$[\text{M}]_{\text{RMC}}$	$k_p/k_{-i}, \text{M}^{-1}$	$\overline{\text{RN}}$	$\text{corr } k_{\text{app}} \times 10^4, \text{s}^{-1}$	$k_p k_i/k_{-i}, \text{M}^{-3} \text{s}^{-1}$	$k_i, \text{M}^{-2} \text{s}^{-1}$	$\Delta T_{\text{max}}, ^{\circ}\text{C}$
Styrene, $-90\text{ }^{\circ}\text{C}$							
8.0	0.34	71.8	42.7	19.4	157	2.2	11.3
7.0	0.33	75.0	46.4	16.7	154	2.1	11.5
6.0	0.31	79.5	51.2	15.5	167	2.1	11.4
5.0	0.28	82.5	56.2	16.3	210	2.6	9.9
4.0	0.25	88.1	63.3	13.9	225	2.6	9.9
3.0	0.22	98.7	74.5	12.1	260	2.6	8.7
2.0	0.18	110.8	89.5	9.0	292	2.6	6.1
Isobutylene, $-90\text{ }^{\circ}\text{C}$							
16.0	0.24	20.0	14.8	261.0	1055	52.8	6.2
14.0	0.21	18.9	14.7	182.1	841	44.4	6.2
12.0	0.18	19.1	15.3	198.4	1070	56.1	7.0
10.0	0.19	23.5	18.7	138.7	897	38.2	5.2
8.0	0.17	26.0	21.3	152.0	1230	47.3	5.8
6.0	0.12	22.5	19.7	83.6	901	40.1	4.7
4.0	0.11	31.2	27.6	67.5	1091	35.0	4.3
2.0	0.06	29.2	27.5	27.2	878	30.1	2.5
1.0	0.03	32.1	31.1	13.1	843	26.3	1.9
0.8	0.02	30.6	29.9	10.1	816	26.7	1.6

<sup>a</sup>  $[\text{Styrene}]_0$  (or  $[\text{IB}]_0$ ) = 0.5 M,  $[\text{DtBP}] = 4.0 \times 10^{-3}$  M,  $[\text{n-Bu}_4\text{NCl}] = 5.0 \times 10^{-4}$  M, and  $[\text{TiCl}_4] = 2.78 \times 10^{-2}$  M; 60/40 MCHex/MeCl cosolvents (v/v).

Table 5. bDCC-Initiated Styrene and IB Rate Constant Data<sup>a</sup>

temp, $^{\circ}\text{C}$	$k_p/k_{-i}, \text{M}^{-1}$	$k_i, \text{M}^{-2} \text{s}^{-1}$	$k_{-i} \times 10^{-7}, \text{s}^{-1}$	$K_{\text{eq}} \times 10^7, \text{M}^{-2}$	$\tau_i, \text{s}$	$\tau_{-i}, \text{ns}$
Styrene						
-60	42.0	1.6	3.6	0.45	798	28
-70	69.5	1.8	2.2	0.84	713	46
-80	91.2	2.3	1.6	1.4	552	61
-90	111	2.6	1.4	1.9	491	74
Isobutylene						
-60	4.3	8.9	16.2	0.55	146	6
-70	9.5	14.7	7.4	2.0	88	14
-80	12.5	20.5	5.6	3.7	63	18
-90	29.1	31.6	2.4	13	41	42

<sup>a</sup>  $[\text{Styrene}]_0$  (or  $[\text{IB}]_0$ ) = 0.5 M,  $[\text{DtBP}] = 4.0 \times 10^{-3}$  M,  $[\text{n-Bu}_4\text{NCl}] = 5.0 \times 10^{-4}$  M, and  $[\text{TiCl}_4] = 2.78 \times 10^{-2}$  M; 60/40 MCHex/MeCl cosolvents (v/v).

for IB polymerizations, larger run numbers for styrene polymerizations (smaller  $k_{-i}$ ), and diffusion-controlled rate constants of propagation for both monomers all indicate that  $k_i$  must be larger for IB polymerization than for styrene polymerization. Using eq 4 and assuming ion pairs are the sole reactive species,  $k_i$  may be calculated from the post-RMC slope of the first-order plot, the value of  $k_p/k_{-i}$  from  $[\text{M}]_{\text{RMC}}$  data, and the known values for  $[\text{I}]_0$  and  $[\text{TiCl}_4]$ . Since the full temperature rise due to the exotherm of RMC had developed within the reactor at this point, the  $k_{\text{app}}$ s were corrected for temperature rise according to the Arrhenius equation, assuming apparent activation energies of  $-3.4$  and  $-7.4$  kcal/mol for styrene and IB, respectively, calculated for  $[\text{bDCC}] = 5.0 \times 10^{-3}$  and  $2.0 \times 10^{-3}$  M, respectively.

Using temperature-corrected  $k_{\text{app}}$ s, listed in Tables 1–4 for both monomers, along with appropriate values for  $[\text{I}]_0$ , and  $[\text{TiCl}_4] = 2.78 \times 10^{-2}$  M, values for  $k_p k_i/k_{-i}$  were obtained for each  $[\text{bDCC}]_0$ , which are also listed in Tables 1–4. Combining  $k_p k_i/k_{-i}$  values with values for  $k_p/k_{-i}$  yielded values for the apparent rate constant of chain-end ionization,  $k_i$ , for styrene and IB, as listed in Tables 1–4. The average values of  $k_i$  from each temperature are listed in Table 5 for both monomers.

As expected, the  $k_i$  values for IB are indeed considerably higher than those of styrene by a factor of 5 at  $-60\text{ }^{\circ}\text{C}$  and 12 at  $-90\text{ }^{\circ}\text{C}$ , which far exceeds  $k_{-i}^{\text{IB}}/k_{-i}^{\text{S}}$  at any temperature. Interestingly, values of  $k_i$  decrease with

increasing temperature for both monomers. Also,  $k_i^{\text{IB}}/k_i^{\text{S}}$  increases with decreasing temperature while  $k_{-i}^{\text{IB}}/k_{-i}^{\text{S}}$  displays the opposite trend. This indicates that  $k_i^{\text{IB}}$  is more sensitive to temperature than  $k_i^{\text{S}}$  and has a larger negative apparent energy of activation. As described above,  $k_i$  is an apparent rate constant, defined as  $k_{\text{iabs}}K_{\text{D0}}$ . Because  $\text{TiCl}_4$  dimerization is exothermic, increases in dimerization must overwhelm decreases in  $k_{\text{iabs}}$  with decreasing temperature, resulting in overall negative apparent activation energies for ionization for both monomers.

Again assuming a value for  $k_p$  of  $1.5 \times 10^9 \text{ M}^{-1} \text{s}^{-1}$  for styrene<sup>12</sup> and  $7 \times 10^8 \text{ M}^{-1} \text{s}^{-1}$  for IB,<sup>11</sup> we calculated average values for  $K_{\text{eq}}$  at each temperature, which are listed in Table 5. As expected, these values are larger for IB polymerizations than for styrene, at each temperature, and appear to be more sensitive to temperature for IB polymerizations than for styrene polymerizations. This is evident by comparing  $k_{\text{app}}$ s for each monomer at  $-60$  and  $-90\text{ }^{\circ}\text{C}$ , as changes in  $k_p$  are minimal. The  $k_{\text{app}}$  measured for styrene increases from  $8.7 \times 10^{-4} \text{ s}^{-1}$  at  $-60\text{ }^{\circ}\text{C}$  to  $19 \times 10^{-4} \text{ s}^{-1}$  at  $-90\text{ }^{\circ}\text{C}$ , a factor of about 2, whereas the  $k_{\text{app}}$  for IB increases from  $4.9 \times 10^{-4} \text{ s}^{-1}$  at  $-60\text{ }^{\circ}\text{C}$  to  $152 \times 10^{-4} \text{ s}^{-1}$  at  $-90\text{ }^{\circ}\text{C}$ , a factor of 31.

Because of significantly smaller values of  $k_i$  and  $k_{-i}$ , the polystyrene chain end is slower to ionize and slower to collapse, resulting in a slower propagation rate and a larger run number compared with IB. The time interval between consecutive ionization events,  $\tau_i$ , equal to  $1/k_i[\text{TiCl}_4]^2$ , and the lifetime of one ionization event,  $\tau_{-i}$ , equal to  $1/k_{-i}$ , for both monomers are listed in Table 5 for each temperature.<sup>8,11</sup> The time interval between ionization events is clearly longer for PS than for PIB chain ends, but the lifetime of ionization is also longer for the PS chain end than for the PIB chain end. As temperature increases, intervals between ionization events become longer and duration of ionization becomes smaller, all due to the effect of temperature on the ionization equilibrium for these two monomers. At colder temperatures,  $k_i$  is larger and  $k_{-i}$  is smaller, shifting the equilibrium of ionization to higher concentrations of active species, resulting in larger run numbers and higher polymerization rates, as illustrated by rate data in Tables 1–4.

**Table 6. Apparent Energies of Activation for  $k_p/k_{-i}$ ,  $k_p k_i/k_{-i}$ , and  $k_i$  for bDCC-Initiated IB and Styrene Polymerizations<sup>a</sup>**

rate constant	E, kcal/mol	
	isobutylene	styrene
$k_p/k_{-i}$	-4.6	-2.4
$k_p k_i/k_{-i}$	-7.8	-3.8
$k_i$	-3.2	-1.3
$k_{app}$	-7.4	-3.4

<sup>a</sup>  $E_{app}$  calculated from  $k_{app}$  vs  $1/T$  plots constructed using  $k_{app}$ s measured under conditions of accurate thermal control over the temperature range -90 to -60 °C.

**Determination of Energies of Activation.** Having determined  $k_p/k_{-i}$ ,  $k_p k_i/k_{-i} = k_p K_{eq}$ , and  $k_i$  over a 30 °C range, the respective apparent energies of activation for these processes,  $E_{p/-i}$ ,  $E_{p \cdot i/-i}$ , and  $E_i$  were calculated from the slopes of  $\ln(k)$  vs  $1/T$  plots, according to the Arrhenius equation. Table 6 lists the activation energies for each process. Also included for reference in Table 6 are the values that we measured for the activation energy of the apparent rate constant of propagation,  $E_{app}$  (from  $k_{app}$ s measured under conditions of accurate thermal control) over the temperature range -90 to -60 °C for styrene and IB. In recent literature, the propagation rate constants for styrene<sup>12</sup> and IB<sup>11</sup> under the present conditions have been reported to be at or near the diffusion limit. This allows one to assume that the activation energy for propagation,  $E_p$ , is approximately zero. Thus, apparent energies of activation for the processes of chain-end deactivation (ion-pair collapse),  $E_{-i}$ , and the chain-end ionization equilibrium,  $E_{eq}$ , may be assigned as follows:  $E_{-i} = -E_{p/-i}$  and  $E_{eq} = E_{p \cdot i/-i}$ .

As discussed earlier,  $E_i$  is negative for both monomers, due to exothermic dimerization of  $TiCl_4$ , and is more highly negative for IB polymerizations than for styrene polymerizations. Since the dimerization equilibrium of  $TiCl_4$  should be unaffected by the identity of the monomer, we can conclude that  $E_{iabs}^S - E_{iabs}^{IB} = 1.9$  kcal/mol; i.e., the activation energy required for ionization of the isobutylene chain end is smaller by about 2 kcal/mol than that for the styrene chain end. The larger negative  $E_i$  for IB is illustrated by more significant changes in intervals between ionization events with temperature than for styrene polymerizations as shown in Table 5.  $E_{-i}$  is larger for IB than for styrene, resulting in greater changes in  $k_p/k_{-i}$  over the temperature range. For example,  $k_p/k_{-i}$  for IB increases by a factor of 6.7 from -60 to -90 °C while that for styrene increases only 2.6 times. Notably,  $E_{eq}$  for IB and styrene, -7.8 and -3.8 kcal/mol, respectively, are very similar to calculated  $E_{app}$ s, -7.4 and -3.4 kcal/mol, respectively, obtained from the slopes of  $\ln(k_{app})$  vs  $1/T$  plots. This confirms that  $E_{app}$  is dominated by the effect of temperature on the ionization equilibrium,  $E_{app} \approx E_i - E_{-i}$ , and  $E_p$  is essentially zero due to diffusion-controlled propagation reaction at low temperatures.

## Conclusions

For quasiling cationic polymerizations of styrene and IB exhibiting the RMC phenomenon,  $k_p/k_{-i}$  was

measured using monomer conversion data acquired from ATR-FTIR according to eq 2. These values, combined with measured  $k_{app}$ s, resulted in the direct calculation of apparent rate constants of chain-end ionization, independently of assumed values for  $k_p$ . Rate constants of ion-pair collapse and apparent ionization equilibrium rate constants were calculated assuming recently reported absolute rate constants of propagation for both monomers. Slower ionization and collapse for quasiling styrene polymerizations compared to IB polymerization were found, where  $k_i^{IB} > k_i^S$  and  $k_{-i}^{IB} > k_{-i}^S$  for the specified temperature range.

From kinetic data at -60, -70, -80 and -90 °C, apparent energies of activation were determined for run number ( $k_p/k_{-i}$ ), apparent propagation ( $k_p k_i/k_{-i}$ ), and chain-end ionization ( $k_i$ ). Assuming that the activation energy for absolute propagation is zero, apparent activation energies for chain-end deactivation ( $k_{-i}$ ) and ionization equilibrium ( $k_i/k_{-i}$ ) were calculated. All processes, and particularly chain-end ionization and deactivation processes, were more dependent on temperature for IB than for styrene.

**Supporting Information Available:** Molecular weight data. This material is available free of charge via the Internet at <http://pubs.acs.org>.

## References and Notes

- Storey, R. F.; Donnalley, A. B.; Maggio, T. L. *Macromolecules* **1998**, *31*, 1523.
- Puskas, J. E.; Lanzendorfer, M. G. *Macromolecules* **1998**, *31*, 8683.
- Puskas, J. E.; Lanzendorfer, M. G.; Pattern, W. E. *Polym. Bull.* **1998**, *40*, 55.
- Storey, R. F.; Donnalley, A. B. *Macromolecules* **2000**, *33*, 53.
- Kennedy, J. P.; Kelen, T.; Tudos, F. J. *Macromol. Sci., Pure Appl. Chem.* **1982-1983**, *A18*, 1189.
- Iván, B. *Makromol. Chem., Macromol. Symp.* **1993**, *67*, 311.
- Puskas, J. E.; Kaszas, G.; Litt, M. *Macromolecules* **1991**, *24*, 5278.
- Storey, R. F.; Thomas, Q. A. *Macromolecules* **2003**, *36*, 5065.
- Breland, K. L.; Smith, Q. A.; Storey, R. F. *Macromolecules* **2005**, *38*, 3026.
- Storey, R. F.; Donnalley, A. B. *Macromolecules* **1999**, *32*, 7003.
- Schlaad, H.; Kwon, Y.; Sipo, L.; Faust, R.; Charleux, B. *Macromolecules* **2000**, *33*, 8225.
- De, P.; Munavalli, M.; Faust, R. *ACS Div. Polym. Chem., Polym. Prepr.* **2003**, *44* (1), 1071.
- Webb, S. P.; Gordon, M. S. *J. Am. Chem. Soc.* **1999**, *121*, 2552.
- Storey, R. F.; Choate, K. R., Jr. *Macromolecules* **1997**, *30*, 4799.
- Kaszas, G.; Puskas, J. E.; Chen, C. C.; Kennedy, J. P. *Macromolecules* **1990**, *23*, 3909.
- Kaszas, G.; Puskas, J. E.; Kennedy, J. P.; Chen, C. C. *J. Macromol. Sci., Pure Appl. Chem.* **1989**, *A26*, 1099.
- Puskas, J. E.; Kaszas, G.; Kennedy, J. P.; Kelen, T.; Tudos, F. J. *Macromol. Sci., Pure Appl. Chem.* **1982-1983**, *A18*, 1229.
- Roth, M.; Mayr, H. *Macromolecules* **1996**, *29*, 6104.
- Mayr, H.; Kuhn, O.; Gotta, M. F.; Patz, M. *J. Phys. Org. Chem.* **1998**, *11*, 642-654.
- Storey, R. F.; Brister, L. B. *ACS Div. Polym. Chem., Polym. Prepr.* **1997**, *38* (2), 287.

MA050470J